Science Advances
AAAS

advances.sciencemag.org/cgi/content/full/6/29/eabb5419/DC1

# Supplementary Materials for

## Crystal structure of the human oxytocin receptor

Yann Waltenspühl, Jendrik Schöppe, Janosch Ehrenmann, Lutz Kummer, Andreas Plückthun*

*Corresponding author. Email: plueckthun@bioc.uzh.ch

Published 15 July 2020, *Sci. Adv.* **6**, eabb5419 (2020)
DOI: 10.1126/sciadv.abb5419

**This PDF file includes:**

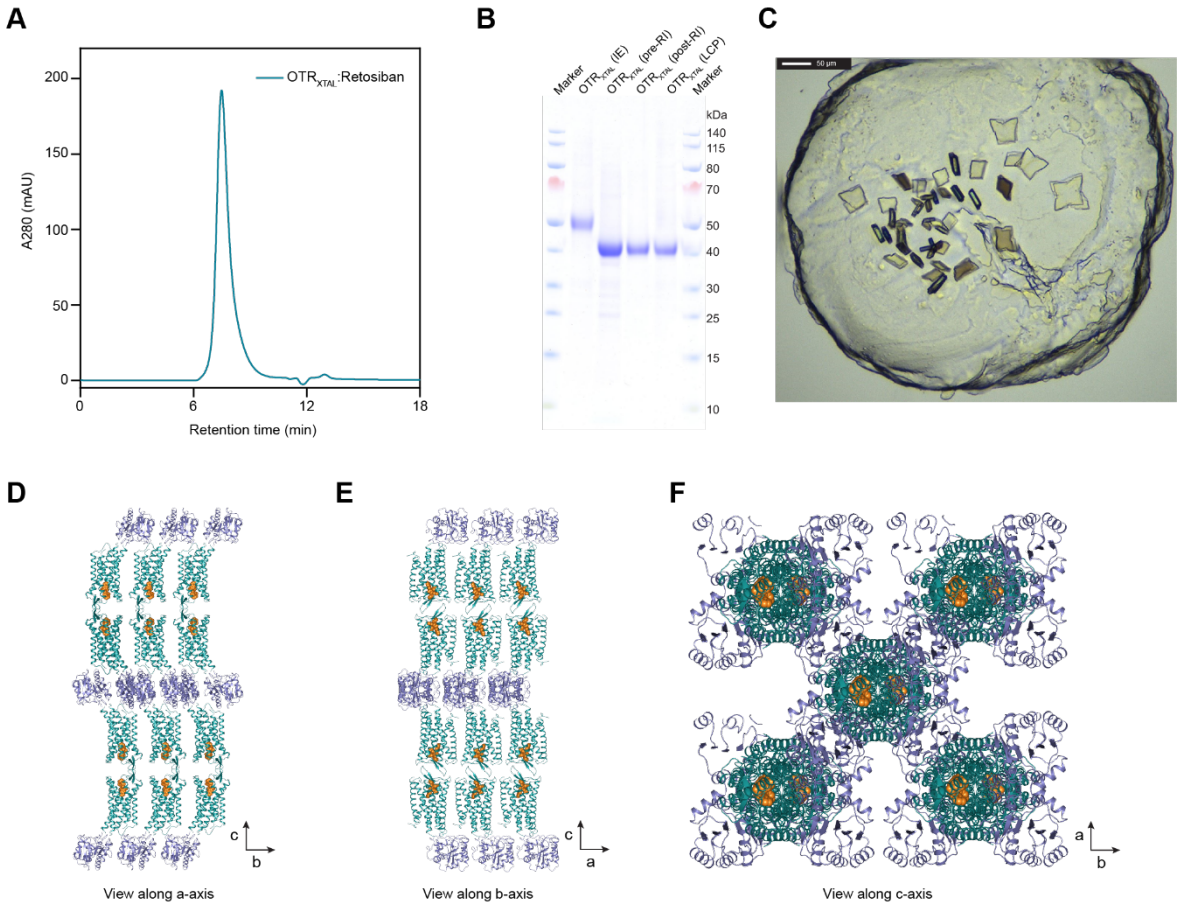


**Fig. S1 | OTR crystallisation**

(**A**) Size exclusion profile of purified OTR:retosiban complex. (**B**) SDS-PAGE gel of purified OTR:retosiban complex. Loading scheme from left to right: IMAC eluate (IE), IMAC eluate after treatment with 3C protease and PNGaseF (pre-RI), reverse IMAC eluate (RI), concentrated reverse IMAC eluate used for crystallisation (LCP). **c**, Bright-field image of OTR:retosiban crystals in lipidic cubic phase. (**C**) Packing of OTR:retosiban crystals as viewed along the a axis of the unit cell. (**D**) Packing of OTR:retosiban crystals as viewed along the b axis of the unit cell. (**E**) Packing of OTR:retosiban crystals as viewed along the c axis of the unit cell.

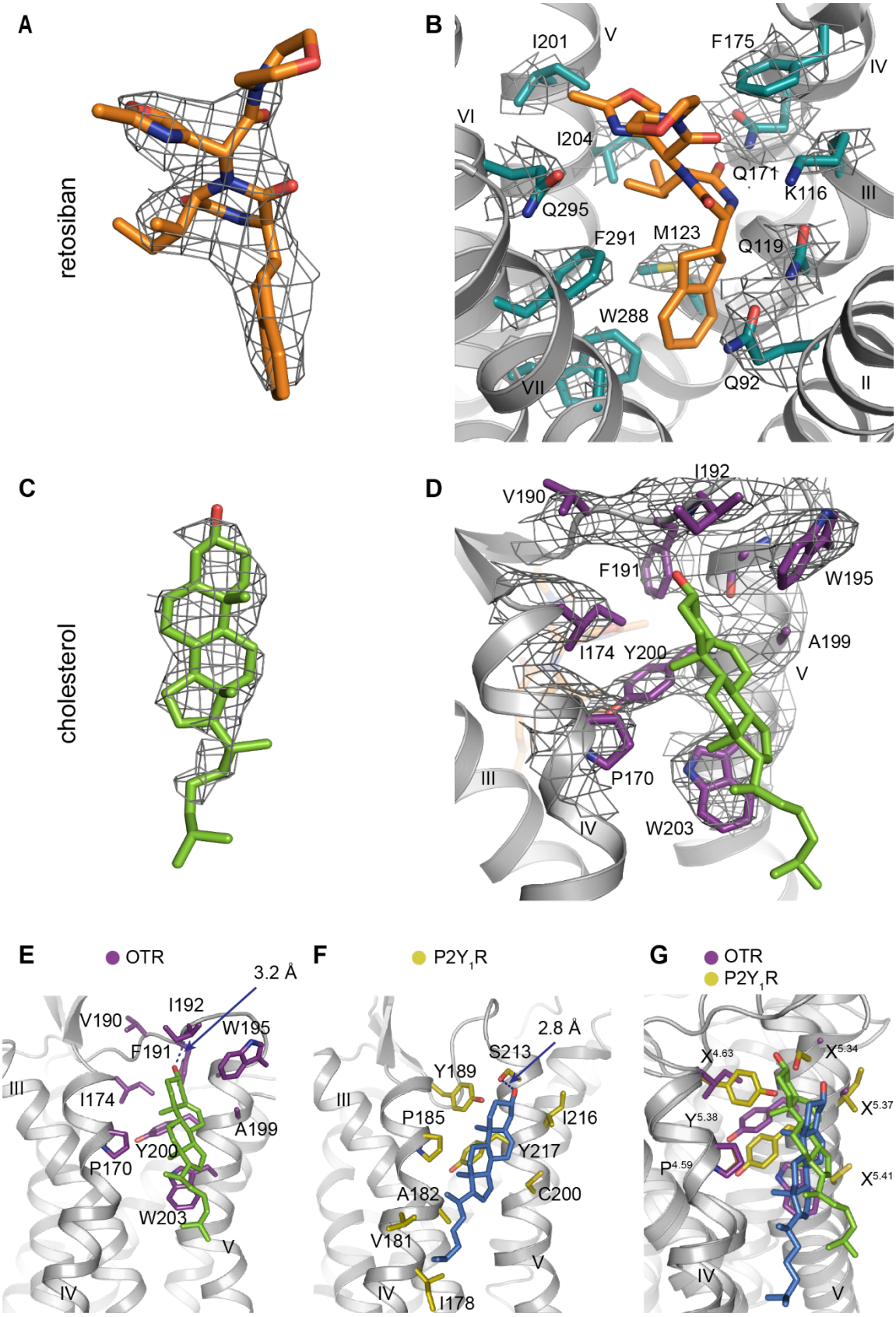
A
retosiban
B
I201
V
F175
IV
VI
I204
Q171
K116
III
Q295
F291
M123
Q119
W288
VII
Q92
II
C
cholesterol
D
I192
V190
F191
W195
A199
I174
Y200
V
P170
III
IV
W203
E
OTR
3.2 Å
I192
V190
W195
F191
III
I174
A199
Y200
P170
W203
V
IV
F
P2Y1R
2.8 Å
S213
Y189
III
P185
I216
Y217
A182
C200
V181
V
IV
I178
G
OTR
P2Y1R
X4.63
X5.34
X5.37
Y5.38
P4.59
X5.41
IV
V

**Fig. S2 | Electron density maps of the extracellular ligand binding pocket the cholesterol binding site of OTR and comparison of cholesterol binding sites of OTR and $P2Y_1R$**

(**A**) Retosiban with 2Fo-Fc electron density map contoured at 1.0 σ. (**B**) 2Fo-Fc electron density map contoured at 1.0 σ for OTR residues interacting with retosiban. Oxygen and nitrogen atoms are coloured in red and blue, respectively. (**C**) Cholesterol with 2Fo-Fc electron density map contoured at 1.0 σ. (**D**) 2Fo-Fc electron density map contoured at 1.0 σ for OTR residues interacting with cholesterol. (**E & F**) Cholesterol binding site of (E) OTR and (F) $P2Y_1R$ (PDB ID: 4XNV) in between transmembrane helices IV and V. Hydrogen bonds are indicated by dashed blue lines. (**G**) Overlay of cholesterol bindings sites of OTR (violet) and $P2Y_1R$ (yellow). Cholesterol molecules are coloured in green (OTR) or in blue ($P2Y_1R$), respectively.

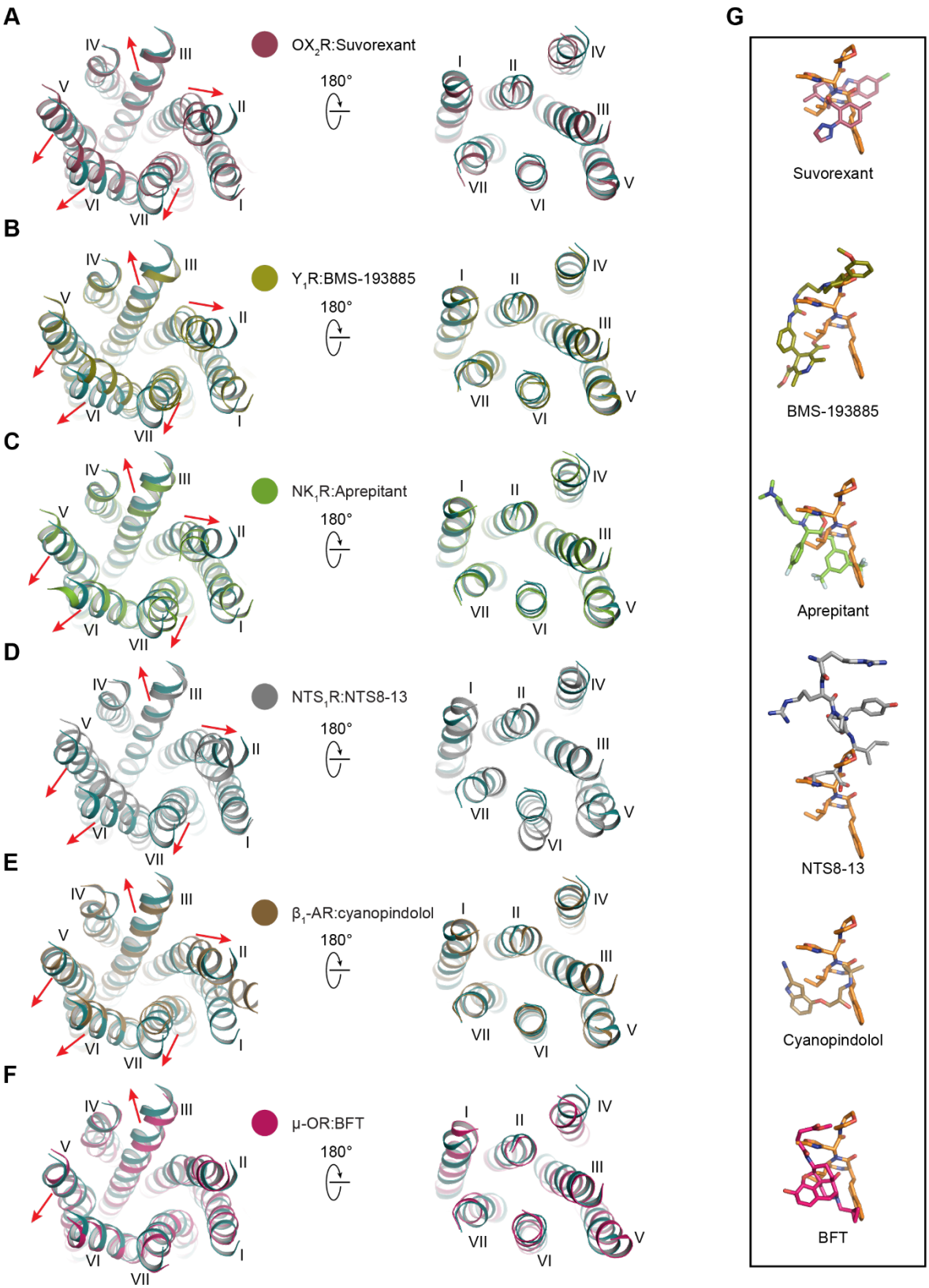
A
OX2R:Suvorexant
180°
B
Y1R:BMS-193885
180°
C
NK1R:Aprepitant
180°
D
NTS1R:NTS8-13
180°
E
β1-AR:cyanopindolol
180°
F
μ-OR:BFT
180°
G
Suvorexant
BMS-193885
Aprepitant
NTS8-13
Cyanopindolol
BFT

**Fig. S3 | Comparison of transmembrane helix conformations shaping the extracellular binding site of OTR to other peptidergic and aminergic GPCRs**

As viewed from the extracellular space (left) and from the cytoplasm (right). Red arrows indicate shift of OTR extracellular helix tips relative to reference receptor.

(**A-F**) Structural superposition of OTR:retosiban (coloured in cyan) with previously reported class A GPCR crystal structures yields root-mean-square deviations (RMSD, summarised in Table S1) for backbone atoms of (A) 2.7 Å to orexin 2 receptor, (B) 2.9 Å to neuropeptide Y Y1 receptor, (C) 1.6 Å to neurokinin 1 receptor, (D) 2.3 Å to neurotensin 1 receptor, (E) 2.6 Å to $\beta_1$-adrenergic receptor and (F) 2.6 Å to the μ-opioid receptor.

(**G**) Isolated ligands from the overlays in (A-F), as viewed from helix VI-VII (retosiban coloured in orange).

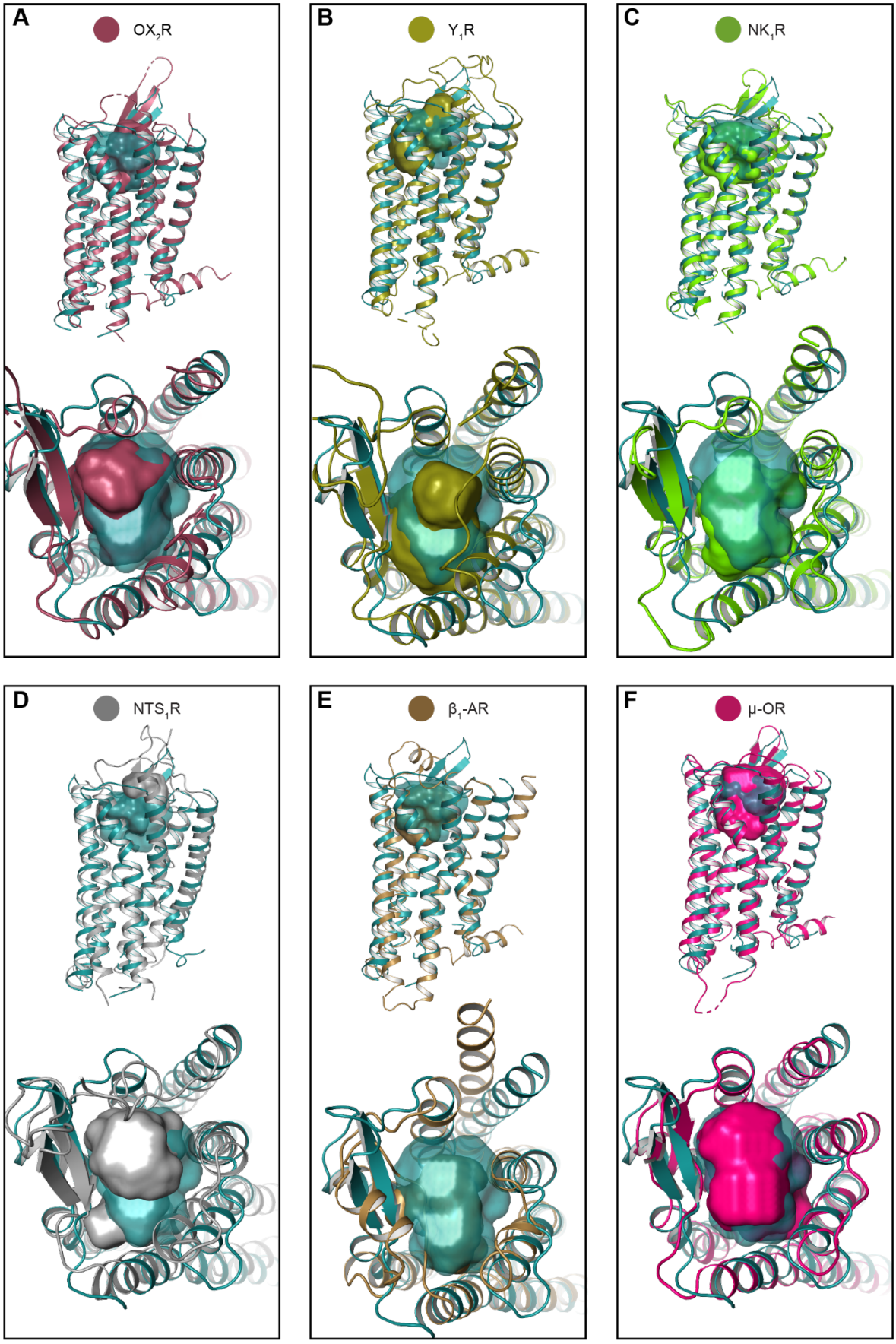
A
OX2R
B
Y1R
C
NK1R
D
NTS1R
E
β1-AR
F
μ-OR

**Fig. S4 | Volume differences of the extracellular binding pocket between OTR and other peptidergic and aminergic GPCRs**

(**A-F**) In each panel an overlay of OTR:retosiban (coloured in cyan) with another GPCR is shown in cartoon representation, as viewed from the membrane plane (top) and from the extracellular space (bottom). The volumes of the extracellular ligand binding pockets are outlined as solid surfaces and highlighted in the respective colour of the receptors. Volumes were calculated using the program POVME 2.0 (Durrant, J.D. *et al*. *J. Chem. Theory Comput.* **10**, 5047-5056 (2014)). The structures overlayed with OTR:retosiban are (A) $OX_2R$:Suvorexant (PDB ID: 4S0V), (B) $Y_1R$:BMS-193885 (PDB ID: 5ZBH), **(**C) $NK_1R$:Aprepitant (PDB ID: 6HLO), (D) $NTS_1R$:NTS8-13 (PDB ID: 4GRV), (E) $\beta_1$ AR:cyanopindolol (PDB ID: 4BVN) and (F) μ-OR:BFT (PDB ID: 4DKL).

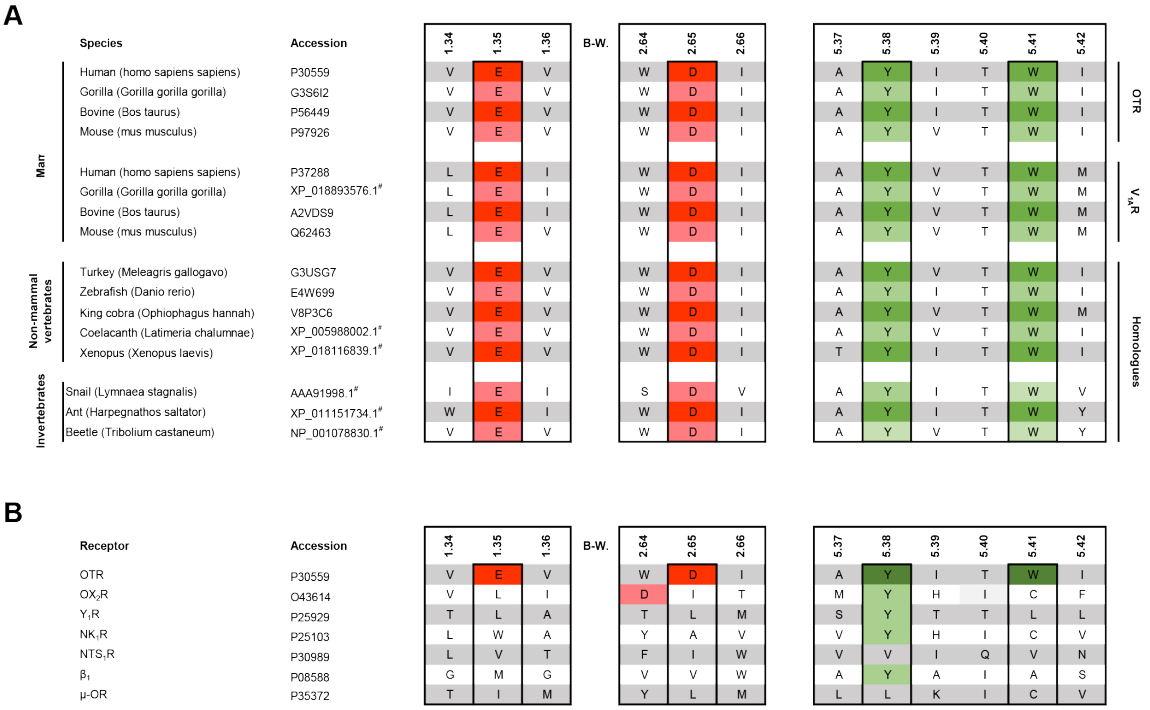


**Fig. S5 | Alignment of the divalent cation binding site of OTR**

(**A**) Amino acid alignment of residues compromising the human OTR divalent cation coordination (red) and cholesterol binding (green) sites and several vertebrate and invertebrate homologues. Species name and UniProt Knowledgebase accession codes (www.uniprot.org) or NCBI reference sequence (marked with #, www.ncbi.nlm.nih.gov) are indicated in the first and second column, respectively. Amino acid residue alignment of positions according to the Ballesteros-Weinstein numbering scheme (BW) are indicated above the sequences. Residues of the OTR magnesium binding site are highlighted by black boxes. Acidic residues are highlighted in red. (**B**) Alignment with other peptidergic and aminergic GPCRs. Receptor name and UniProt Knowledgebase (www.uniprot.org) accession codes are indicated in the first and second column, respectively. Amino acid residue alignment of positions 1.34-1.36 and 2.64-2.66 according to the Ballesteros-Weinstein numbering scheme (BW) are indicated above the

sequences. Residues of the OTR magnesium binding site are highlighted by black boxes. Acidic residues are highlighted in red.

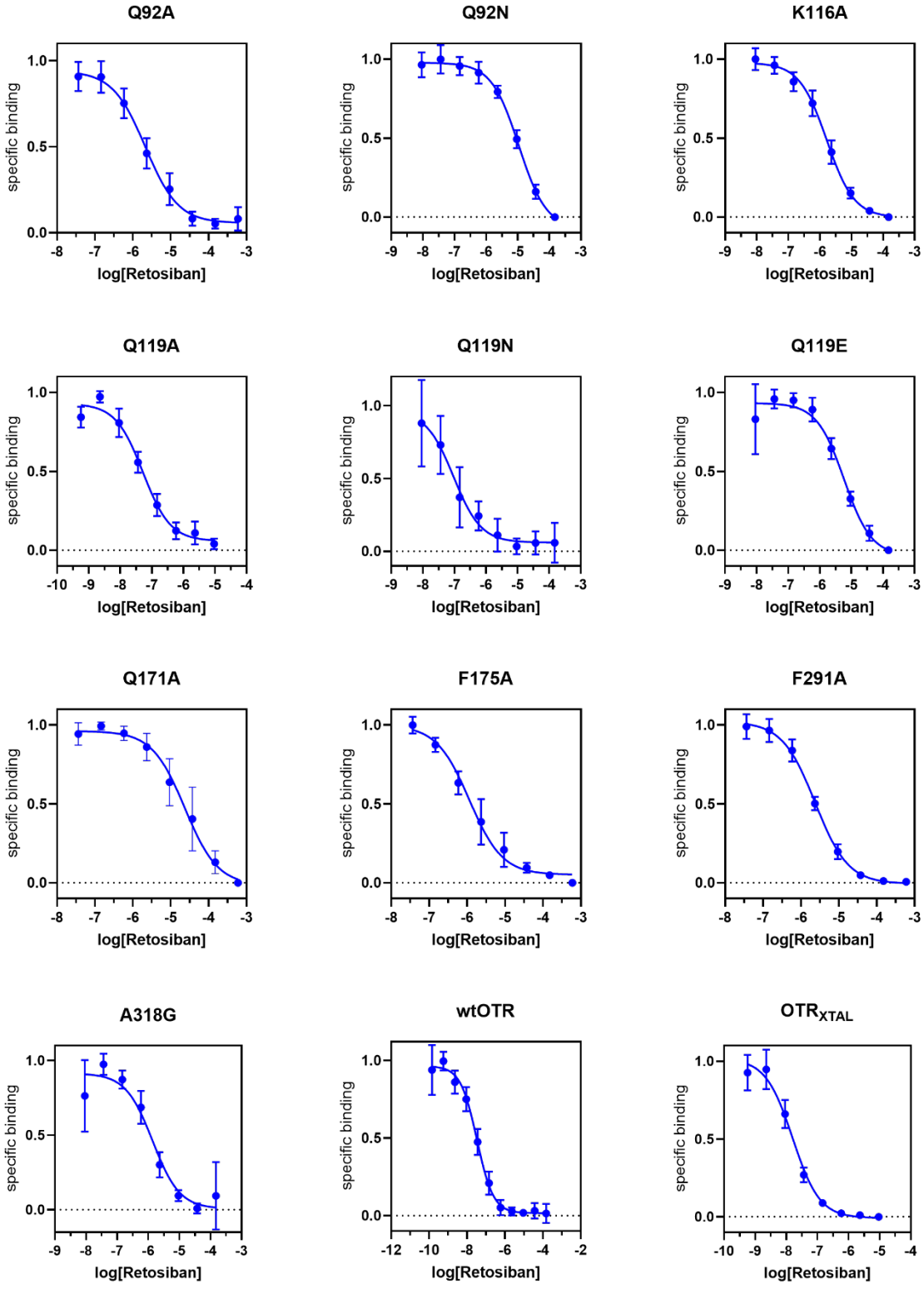
Q92A
Q92N
K116A
Q119A
Q119N
Q119E
Q171A
F175A
F291A
A318G
wtOTR
OTR$_{XTAL}$
specific binding
log[Retosiban]

**Fig. S6 | Binding of retosiban to wild-type and mutated OTR variants**

Whole-cell competition binding experiments of different concentrations of unlabelled retosiban to HEK293T cells expressing wild-type (wtOTR) and mutated wtOTR variants, in the presence of fluorescently labelled PVA as a competitor. Binding curves are shown with 95% confidence intervals (CI) from 3 independent experiments performed as quadruplicates

**Table S1 | Extracellular ligand binding pocket comparison.**

| receptor | RMSD [Å] | ligand | $M_w$ [g $mol^{-1}$] | pocket volume [$Å^3$] | pocket volume relative to OTR [%] | PDB ID |
|---|---|---|---|---|---|---|
| OTR | | retosiban | 494.6 | 792 | 100 | xx |
| OX2R | 2.7 | Suvorexant | 450.9 | 569 | 72 | 4S0V |
| $Y_1R$ | 2.9 | BMS-193885 | 590.7 | 605 | 76 | 5ZBH |
| $NK_1R$ | 1.6 | Aprepitant | 534.4 | 597 | 75 | 6HLO |
| $NTS_1R$ | 2.3 | NTS8-13 | 817.0 | 433 | 55 | 4GRV |
| $\beta_1$-AR | 2.6 | Cyanopindolol | 287.4 | 320 | 40 | 4BVN |
| μ-OR | 2.6 | BFT | 468.5 | 911 | 115 | 4DKL |

Root-mean-square deviations for backbone atoms (RMSD). Pocket volumes were calculated using the program POVME 2.0 (Durrant, J.D. *et al*. *J. Chem. Theory Comput.* **10**, 5047-5056 (2014)).

**Table S2 | Binding of retosiban to wild-type and mutated OTR variants.**

| construct | $K_i$ retosiban [nM] | 95% CI [nM] | $K_D$ PVA-HL647 [nM] | $B_{max}$ [%wtOTR] |
|---|---|---|---|---|
| Q92A | 16.3 | 11.7 - 22.7 | 0.20 ± 0.12 | 6.9 ± 2.7 |
| Q92N | 517.6 | 411.1 - 650.8 | 0.32 ± 0.21 | 25.6 ± 0.4 |
| K116A | 195.4 | 158.4 - 241.3 | 0.84 ± 0.43 | 38.7 ± 0.1 |
| Q119A | 2.2 | 1.7 - 3.0 | 4.0 ± 1.1 | 9.1 ± 2.5 |
| Q119N | 31.1 | 11.1 - 85.4 | 2.8 ± 1.5 | 11 ± 0.2 |
| Q119E | 1142.9 | 767.3 - 1713 | 1.4 ± 0.46 | 33.1 ± 0.7 |
| M123A | n.b. | | n.b. | n.b. |
| Q171A | 8260.4 | 5221 - 13060 | 88.5 ± 19.8 | 211.3 ± 59 |
| F175A | 11.7 | 8.9 - 15.3 | 199 ± 8.2 | 101.5 ± 43.9 |
| I201A | n.b. | | n.b. | n.b. |
| I204A | n.b. | | n.b. | n.b. |
| F291A | 1078.9 | 897.1 - 1299 | 21.9 ± 5.7 | 78.7 ± 19.5 |
| A318G | 40.5 | 25.2 - 65.3 | 0.38 ± 0.16 | 11.4 ± 0.3 |
| wtOTR | 2.6 | 2.0 - 3.3 | 0.58 ± 0.25 | 100 ± 26.3 |
| $OTR_{XTAL}$ | 7.6 | 5.9 - 9.9 | 6.4 ± 3.3 | 387 ± 48.9 |

Whole-cell competition binding experiments of different concentrations of unlabelled retosiban to HEK293T cells expressing wild-type (wtOTR) and mutated wtOTR variants, in the presence of fluorescently labelled PVA as a competitor. Retosiban affinities are shown as mean values ($K_i$) with the respective 95% confidence intervals (CI) from 3 independent experiments performed in quadruplicates. *n.b.*, no binding. $K_i$ values were calculated using the Cheng-Prusoff equation (Cheng, Y. & Prusoff, W.H. *Biochem. Pharmacol.* **22**, 3099-108 (1973)). PVA-HL647 saturation binding results to individual receptor variants are reported as $K_D$ and $B_{max}$ ± standard deviation from at least 3 independent experiments, each performed in triplicates.

**Table S3 | Binding of agonist or antagonist to wild-type OTR and variants with mutations in the cholesterol binding site.**

| construct | surface expression [% of wtOTR] | $B_{max}$ agonist [% of wtOTR] | $B_{max}$ antagonist [% of wtOTR] |
|---|---|---|---|
| Y200A | 111.3 ± 17.1 | 4.6 ± 4.1 | 0.7 ± 0.03 |
| Y200H | 108.0 ± 13.3 | 11.7 ± 1.5 | 3 ± 0.4 |
| W203A | 104.5 ± 16.5 | 19.2 ± 3.5 | 8.1 ± 0.5 |
| W203H | 101.3 ± 27.5 | 5.1 ± 1.5 | 0.2 ± 0.02 |
| wtOTR | 100 ± 13.9 | 100 ± 20.5 | 100 ± 3.5 |
| $OTR_{XTAL}$ | 182.7 ± 38.5 | 471.4 ± 50.4 | 419.7 ± 44.2 |

Whole-cell specific binding experiments of agonist (HL488-$Orn^8$-OT) and antagonist (HL647-PVA) on HEK293T cells expressing wild-type (wtOTR) and mutated wtOTR variants expressed as $B_{max}$ values. In comparison the surface expression is also shown. Data are shown as mean values (surface expression and $B_{max}$) ± standard deviations (SD) from 3 independent experiments performed in triplicates.

**Table S4 | Thermostability of $OTR_{XTAL}$ and variants with mutations in the cholesterol binding site.**

| construct | $T_m$ + CHS [°C] | $T_m$ - CHS [°C] |
|---|---|---|
| $OTR_{XTAL}$ Y200A | 55.2 ± 0.8 | 44.5 ± 3.9 |
| $OTR_{XTAL}$ W203A | 61.2 ± 0.2 | 41.9 ± 3.1 |
| $OTR_{XTAL}$ | 64.2 ± 0.6 | 43.7 ±1.9 |

CPM thermostability assay of $OTR_{XTAL}$ and mutated variants thereof in the presence or absence of the cholesterol analogue cholesteryl hemisuccinate (CHS). Data are shown as mean values ($T_m$) ± standard deviations (SD) from 3 independent experiments.

**Table S5 | Ligand binding to wild-type OTR and variants with mutations in the $Mg^{2+}$ binding site.**

| construct | $Mg^{2+}$ | $K_D$ [nM] | 95% CI [nM] |
|---|---|---|---|
| wtOTR | + | 1.2 | 0.9 - 1.5 |
| wtOTR | – | 27.9 | 22.7 - 34.4 |
| E42A | + | 19.1 | 15.0 - 24.4 |
| E42A | – | 29.6 | 23.0 - 38.4 |
| D100A | + | 26.2 | 23.8 - 28.8 |
| D100A | – | 30.8 | 28.1 - 33.7 |
| E42D, D100E | + | 16.4 | 11.2 - 24.1 |
| E42D, D100E | – | 28.4 | 20.1 - 40.7 |

Whole-cell specific binding experiment of agonist (HL488-$Orn^8$-OT) to HEK293T cells expressing wild-type (wtOTR) and mutated wtOTR variants in the presence (+) or absence (-) of 3 mM $Mg^{2+}$. Data are shown as mean values ($K_D$) with the respective 95 % confidence interval (CI) from three independent experiments performed in triplicates.